

Answer to anonymour Referee #1

I thank the reviewer for his/her constructive comments. According to your reviews, I rearranged the manuscript and answered your questions as follows.

Reviewer quote 1: While I understood the second type of flood, it is not clear the first type. Please, clarify it (P2, L16-19)

Answer 1: To explain the first type of flood, I added a sentence “In the first type, river basins respond rapidly to intense rainfall because of steep slopes, impermeable surfaces, saturated soils, or because of anthropogenic forcing to the natural drainage” to the second paragraph of the introduction section.

Reviewer quote 2: I think the comparison is between Figure 4a and 9: can you show them with the same colour legend in the investigated area? The differences between models and observations would be better appreciated (P6,L3).

Answer 2: Thanks for your comments. In accordance with your explanations, I rearranged Fig. 4a colour legend similar that of Fig. 9.

Reviewer quote 3: When you say: “Optimum spatial coverage...” It’s difficult to spot with different maps and colours. (P12-L4).

Answer 3: As you mentioned above, it can be difficult to distinguish the optimum spatial coverage. However, when we focused on the spatial distribution of the measured precipitation (Fig. 4a) data, we can see the highest daily precipitation totals are only shown in the seaside stations of Artvin and the other two NWP model forecasts do not well coincide with observation values.

Reviewer quote 4: Please, add some references about the NWP models, in particular some physics features about the WRF (used version) and the ALARO models (P5, Section 2.3)

Answer 4: To give more details of the physics of the NMM-WRF, I added some sentences at the end of the first paragraph of the Section 2.3 as follows:

“The mesoscale NWP system of Non-hydrostatic Mesoscale Model (NMM) core of the Weather Research and Forecasting (WRF) is developed by the National Oceanic and Atmospheric Administration (NOAA)/National Centers for Environment Prediction (NCEP), NMM-WRF is a fully compressible, non-hydrostatic mesoscale model with a hydrostatic option (Janjic, 2003). The model uses a terrain-following hybrid sigma-pressure vertical coordinate. The grid staggering is the Arakawa E-grid. The model uses a forward-backward scheme for horizontally-propagating fast waves, an implicit scheme for vertically-propagating sound waves, the Adams-Bashforth scheme for horizontal advection, and the Crank-Nicholson scheme for vertical advection. The dynamics conserve a number of first and second order quantities including energy and enstrophy.”

For the Alaro model, a brief explanation together with its references was added to the Section 2.3 as follows:

“For the regional weather forecasts, the Alaro meteorological model has been designed to be run at convection-permitting resolutions. The key concept is in the precipitation and cloud scheme called Modular Multiscale Microphysics and Transport (3MT) developed by Gerard and Geleyn (2005), Gerard (2007), and Gerard et al. 2009. In the usage of the Alaro by TSMS, whereas the outer domain has grid spacing of 10 km, the inner domain has almost 5 km of grid spacing as well as 60 vertical levels.”

Reviewer quote 5: What do you mean with “moderate climates”? (P6, L13)

Answer 5: “Moderate climates” were changed to “more dry climates” term in the text.

Reviewer quote 6: you wrote:”the highest amount of precipitation is observed during wet and dry seasons”. It confuses me: how could it be in dry season, if we are talking of the highest amount?

Answer 6: “... In terms of precipitation values,...” sentence was rephrased and instead, “When compared with the other regions, highest winter and summer precipitation totals are observed in this part of Turkey due to the interactions of synoptic weather patterns and orographic lifting.” term was added.

Technical corrections:

P1, L22: I suggest: “...flood damages in the Artvin area.” [It was corrected.](#)

P2, L5-10: I suggest: “For example, just one flash flood in 2002...” [It was corrected.](#)

P2, L9: I suggest: “For example, just a single flash flood caused €1.2 billion Euro damages in the Gard region of France in 2002 (Huet et al., 2003), €300 million Euro damages in the Pinios (Greece) flash flood during 1994 (Gaume et al., 2008), €65 million Euro economic losses in the Magorala (Spain) flash flood in 2000 (Llasat et al., 2001), and €4.6 million Euro in the 2007 Mastroguglielmo (Italy) flash flood event (Aronica et al., 2008). [It was corrected.](#)

P3, L9: Remove “a” before “slow-moving” [It was corrected.](#)

P3, L13: I suggest “triggered landslides” [It was corrected.](#)

P3, L16: Remove “the” before “rainfall” [It was corrected.](#)

P4, L7: Remove the apostrophe after “dollars” [It was corrected.](#)

P5, L2: I suggest “meteorological stations” [It was corrected.](#)

P5, L4: I suggest: “and to” instead of “as well as” [It was corrected.](#)

P5, L9: I suggest “as the previous day atmospheric...” [It was corrected.](#)

P5, L19: I suggest: “In the Alaro meteorological model...” [It was corrected.](#)

P6, L16: I suggest: “due to...” instead of “because of...” [It was corrected.](#)

P7, L4: I suggest to replace “instead of” with “while” [The sentence was rearranged.](#)

P7, L9-10: I suggest to remove this sentence: “Nevertheless...” [It was corrected.](#)

P7, L16: Replace “those” with “the” [It was corrected.](#)

P8, L2: Replace: to with “from” [It was corrected.](#)

P8, L3: Do you mean “dropping from 4 to 2”? [It was corrected.](#)

P8, L7: I suggest: “The maximum daily precipitation value was...” [It was corrected.](#)

P9, L6: I suggest: “eastern” instead of “east to” [It was corrected.](#)

P9, L9: “and through the axis”: this sentence is not clear, please clarify it. [The sentence was rearranged.](#)

P9, L16: add “the before “moving”. Remove semicolon after “thus” [It was corrected.](#)

P10, L5: “(not shown)”: do you mean not shown in the text? [Temp diagram was not shown](#)

P10, L19: I suggest “the storm intensity” It was corrected.

P12, L1: I suggest: to the Alaro model” It was corrected.

P12, L10: I suggest “issue” instead of “give” It was corrected.

P12, L20: I suggest “6 to 7 hours” It was corrected.

P13, L12: I suggest to move this sentence at the beginning of the conclusion section. Done

P20, L6: I suggest: “in °C)” It was corrected.

Answer to anonymour Referee #2

Thanks a lot for your valuable comments for the manuscript. According to your comments related to precipitation climate of region and comparison with the other region, I gave detail information for the seasonal precipitation distribution and synoptic and orographic mechanisms that cause precipitation, and I gave a reference to emphasis the awareness of the regional precipitation than the other regions precipitation distribution in Section. 3.1. Also, in the direction of your comments, my manuscript was sent to a native English speaker and some grammatical errors were rearranged.

Answer to anonymour Referee #3

I thank the reviewer for his/her constructive comments. According to your reviews, I rearranged the moderate and minor points as follows:

Moderate Points:

Reviewer quote 1: At the end of abstract, I recommend one sentence as a take-home message (general message)

Answer 1: According to your comments, i added “This study supports conventional weather analysis, satellite images, and forecast model output to alert forecasters to the potential for heavy rainfall.” Sentence at the end of the abstract.

Reviewer quote 2: Similarly, in the Conclusion Section, please add a few sentences as a take-home message for decision makers to emphasize the applicability of the outcomes of this study

Answer 2: At the end of the Conclusion Section, “The synoptic and atmospheric descriptions give better knowledge of the mesoscale convective systems and the mechanisms driving torrential rains in the EBS. It is hoped that more detailed studies will be performed on synoptic development leading to extreme summer precipitation events in EBS.” Sentence was corrected and added.

Minor Points:

P1. L12. ...total accumulated rainfall AMOUNTS of 136, 69, and 109 mm WERE measured. . . . It was corrected.

P1. L22. Delete ‘the’ before Artvin. Done.

P2. L2. Insert ‘the’ before warm.on THE warm Mediterranean Sea. . . . Done.

P2. L6. Delete ‘the’ before 2002. Done.

P2. L6. Delete Euro sign (. . . .caused 1.2 billion damages. Similar, also correct: P2.L7, P2.L8, P.2L9. . . . Done

P2. L9. Delete ‘the’ before 2000. . . .flood in 2000. . . . Done.

P2. L10. WORD CHOICE. My recommendation:it is necessary to IMPROVE OUR CURRENT UNDERSTANDING about the. It was corrected.

P2. 16. Re-write. My recommendation: Depending on the catchment characteristics, mainly two types of flood occur in Turkey. It was corrected.

P2. L18. COMMA. Insert a comma after ‘affected’. Done

P2. L18. CAPITALIZATION. Capitalize ‘river’. . . .of the Meric River. . . . Done.

P3. L5. Re-write. My recommendation: . . .in Antalya, a coastal city located on the Mediterranean Sea. Done.

P3. L8. Re-write. My recommendation:investigated the hydrometeorological role of floods occurred during 7-10 September, 2010 in the Marmara Region. Done.

P3. L15-17. Re-write. My recommendation: The underlying geology of the EBS is generally consists of semi-permeable volcanic rocks which reduce infiltration and enhance runoff production (XXXX). It was corrected.

P3. L17-19. Re-write. My recommendation: The north-eastern coastal parts of Turkey, regions located on the windward slopes of the EBS facing the Black Sea, receives more than 2000 mm of annual precipitation which is the wettest part of the country. It was corrected.

P3. L19-21. Re-write. My recommendation: The large mountainous area which extends through the Black Sea, and slope instability due to steep gradients as well as intense rainfall

result in flash floods and landslides and threaten the settlements in the EBS region. [It was corrected.](#)

P4. L1. VERB. . . .facilitate. . . [Done.](#)

P4. L7. TYPO at the end of dollars. . . .dollars' Delete the apostrophe. [Done.](#)

P4. L8. WORD CHOICE. . . .the DETRIMENTAL EFFECTS of floods for. . . [Not changed](#)

P4. L11. WORD CHOICE. . . .the aim of this research is TO FOCUS on. . . [Not changed](#)

P4. L20. Insert a comma after synoptic. . . .synoptic, and . . . [Done.](#)

P4. L22. WORD CHOICE. . . .with WEATHER forecasts. . . [Done.](#)

P5. L4. Insert 'to' before retrieve. . . .as well as TO retrieve. . . . [Done](#)

P5. L16-19. Re-write. [Section 2.3 was rewritten according to the comments of the Reviewer 1.](#)

P6. L2. Insert a comma after 'domain'. . . .domain, and . . . [Done](#)

P6. L9. Re-write. My recommendation: This mountain chain extends parallel to the Black Sea and . . . [Done](#)

P6. L11-12. Re-write. My recommendation: . . .the region also experiences orographic effect on precipitation. [Not changed](#)

P6. L14-15. Re-write. My recommendation: The rain shadow effect on the lee side of the mountainous area CAUSES a more. . . [Done](#)

P7. L2. WORD CHOICE. . . .(MAP) VARIES from. . . . [Done](#)

P7. L6. Explain MCS. Describe acronym 'MCS'. [It was explained in Introduction Section](#)

P7. L7. WORD CHOICE. . . .were OBSERVED AT Hopa, Rize, and Pazar with . . . [Done](#)

P7. L13. Insert a comma after 'Hopa'. . . .Hopa, and . . . [Done](#)

P7. L17. Insert a comma after 'Arhavi'. . . .Arhavi, and . . . [Done](#)

P7. L20. WORD CHOICE. . . .Another coastal station, Arhavi. . . [Done](#)

P7. L22. Re-write. Describe it. Temporal distribution of WHAT?

Temporal distribution of XXXXXXXX that. . . . [It was corrected by adding "precipitation" after Temporal](#)

P8. L1. Insert 'THE' before midday.at THE midday on the. . . [Done](#)

P8. L2. REPLACE. Hourly observations AT the three stations. . . [Done](#)

P8. L2. REPLACE. . . .increased FROM 27 to 32. . . [Done](#)

P8. L3. REPLACE. . . .DROPPED to 2-4 mm. . . [Done](#)

P8. L6. DELETE 'station'. . . .at Hopa during. . . . [Done](#)

P8. L19 CHECK. I am not sure 'phenomenology' is the correct word there? [Not changed](#)

P9. L4-7. Re-write. (Azarbijan). Make sure that a reader should understand that Azerbaijan is another country that locates east of Turkey. [Not changed](#)

P9. L17-18. Re-write. My recommendation: . . .with a decrease in temperature from . . . [Done](#)

P10. L1. VERB. . . .that developed severe. . . . [Done](#)

P10. L4. REPLACE. . . .activity before and during [Done](#)

P10. L11. . . .were used to examine THE ATMOSPHERIC CONDITIONS ON 24 August. . . [Done](#)

P10. L17-19. Re-write. You do not need to say more yellowish. On the other hand, more intense storms were observed over the land areas such as Georgia (Fig.7a). [Done](#)

P11. L5. WORD CHOICE. . . .was investigated IN DETAIL by. . . [Done](#)

P11. L9. WORD CHOICE. . . .the role of SSTs of the Black Sea on. . . . [Not changed](#)

P11. L10. INSERT 'the'. . . .for THE BS. . . [Done](#)

P11. L12. WORD CHOICE. . . .were NORTH OF the latitude of 44°N. [Done](#)

P11. L13. VERB TENSE. Use PAST TENSE. . . .exceedED [Done](#)

P11. L14. WORD CHOICE. . . . values in NORTH OF 44°N latitude. [Done.](#)

P11. L20. VERB TENSE.station observations WERE clearly. . . . [Done.](#)

P12. L1. Describe Alaro model. [Detail description of the Alaro were given in Section 2](#)

P12. L5-7. Re-write the sentence. [Not changed](#)

P12. L12. VERB TENSE. . . .offices GAVE alert messages.instead of GAVE,
I used issued term.

P12. 14. Insert a comma after 'Artvin'. . . .Artvin, and Trabzon. . . Done.

P13. L7. WORD CHOICE. . . .was transported FROM THE SEA to the atmosphere. Done.

Figure 1. Narrower region for Turkey map. Show Georgia and Azerbaijan as countries. Not changed

Figure 2. In the caption: Hopa CITY centre. . . . Done.

Figure 4. In the caption: . . .in THE eastern Black Sea. . . . Done.

Figure 5. In the caption: I recommend using following:units in g kg-1). . . . Done

Figure 5. L7. Insert a space after 2015, 00:00 UTC. . . . Done.

Figure 8. L2. Mean of August. . . Done.

L3.over THE Black. . . . 24 August. . . Done.

L4. . . .long-term Augustdata ARE derived. . . . Done.

Figure 9. Delete comma after region. . . .region (a) for. . . . Done.

1 **Meteorological analysis of flash floods in Artvin (NE Turkey) on**

2 **August 24, 2015**

3 **Hakki Baltaci^{1*}**

4

5 ¹ Turkish State Meteorological Service, Istanbul, Turkey

6 * Corresponding author. email: baltacihakki@gmail.com

7 Tel: +90 2164573400 Fax: +90 2164573403

8

9

Abstract

On August 24, 2015 intense rainfall episodes generated flash floods and landslides on the eastern Black Sea coast of Turkey. As a consequence of the heavy rainstorm activity over Artvin and its surroundings (NE Turkey), 11 people died and economic losses totaled a million dollars. During the six hours of the event (from 05:00 UTC to 11:00 UTC), total accumulated rainfall amounts of 136, 64, and 109 mm were measured in the Hopa, Arhavi, and Borçka settlements of Artvin city, respectively. This study comprehensively investigates the meteorological characteristics of those flash floods. In terms of synoptic mechanisms, the cut-off surface low from the summer Asian monsoon settled over the eastern Black Sea. After two days of quasi-stationary conditions of this cyclone, sea surface temperatures (SSTs) reached 27.5 °C (1.5 °C higher than normal) and low-level moisture convergence developed. In addition, transfer of moisture by warm northerly flows from the Black Sea and relatively cool southerly flows from the land coasts of the Artvin district exacerbated the unstable conditions, and thus, played a significant role in the development of deep convective cells. Severe rainstorms as well as the slope instability of the region triggered landslides and worsened flood damages in Artvin area. This study supports conventional weather analysis, satellite images, and forecast model output to alert forecasters to the potential for heavy rainfall.

Keywords: eastern Black Sea; Artvin; flash flood; mesoscale convective systems; Turkey

mac baltaci 20/5/2017 01:13

Deleted: as

mac baltaci 20/5/2017 01:14

Deleted: the

mac baltaci 16/5/2017 01:28

Deleted: district

35

36

37 1. Introduction

38 The interaction between mesoscale convective systems (MCS) on the warm
39 Mediterranean Sea and sudden orographic lifting in the coastal regions produces severe
40 precipitation in the Mediterranean countries (Rebora et al., 2012). These severe
41 precipitation events generally generate flash floods and cause serious damages and
42 economic losses. For example, just a single flash flood caused 1.2 billion Euro damages in
43 the Gard region of France in 2002 (Huet et al., 2003), 300 million Euro damages in the
44 Pinios (Greece) flash flood during 1994 (Gaume et al., 2008), 65 million Euro economic
45 losses in the Magorala (Spain) flash flood in 2000 (Llasat et al., 2001), and 4.6 million
46 Euro in the 2007 Mastroguglielmo (Italy) flash flood event (Aronica et al., 2008). Due to its
47 huge social and economic impacts, it is necessary to improve our current understanding
48 about the spatio-temporal dynamics of flash floods to improve their forecast and the land-
49 use planning. For this reason, several studies have analyzed the meteorological (e.g. Milelli
50 et al., 2006; Fragoso et al., 2012), hydrological (e.g. Silvestro et al., 2012) or
51 hydrometeorological (e.g. Delrieu et al., 2005; Borga et al., 2007) characteristics of floods
52 at a particular area and time.

53 Depending on the catchments characteristics, mainly two types of flood occur in
54 Turkey. In the first type, river basins respond rapidly to intense rainfall because of steep
55 slopes, impermeable surfaces, saturated soils, or because of anthropogenic forcing to the
56 natural drainage. As a consequence of this type flooding, large areas are affected, and
57 economic losses are considerable (e.g. the overflow of the Meriç River in NW Turkey). The

- mac baltaci 16/5/2017 01:32
Deleted: only
- mac baltaci 16/5/2017 01:32
Deleted: one
- mac baltaci 16/5/2017 01:32
Deleted: in the 2002
- mac baltaci 23/5/2017 12:03
Deleted: €
- mac baltaci 23/5/2017 12:03
Deleted: €
- mac baltaci 23/5/2017 12:03
Deleted: €
- mac baltaci 16/5/2017 01:33
Deleted: the
- mac baltaci 23/5/2017 12:03
Deleted: €
- mac baltaci 23/5/2017 12:05
Deleted: increase our knowledge
- mac baltaci 23/5/2017 12:08
Deleted: In Turkey,
- mac baltaci 23/5/2017 12:08
Deleted: s
- mac baltaci 23/5/2017 12:08
Deleted: generally
- mac baltaci 23/5/2017 12:07
Deleted: , depending on the catchments characteristics
- mac baltaci 16/5/2017 02:18
Deleted: a
- mac baltaci 16/5/2017 02:19
Deleted: in river basins
- mac baltaci 20/5/2017 01:17
Deleted: r

75 second type, which is more common, is when flash floods are suddenly triggered by severe
76 rainstorms in certain areas (e.g. coastal regions of the country). In this context, numerous
77 studies have investigated the meteorological role in the occurrence of flash floods in
78 different parts of Turkey. Kömüştü et al. (1998) analyzed the meteorological and terrain
79 features of the flash flood that occurred on November 3 and 4, 1995 on the Aegean coast,
80 when 61 people died in İzmir (western Turkey). They emphasized that low-level advection,
81 positive vorticity, and strong upper-level divergence together with a squall line oriented
82 NE-SW over the Aegean Sea exacerbated the storm. Subsequently, Kotroni et al., (2006)
83 investigated the storm activity that occurred on December 5, 2002 in Antalya, a coastal city
84 located on the Mediterranean Sea. They found that warm and moist air masses driven by a
85 low-level jet as well as orographic barriers caused more than 230 mm of 24-h accumulated
86 precipitation during the event. Later, Kömüştü and Çelik (2013) investigated the
87 hydrometeorological role of floods occurred during 7-10 September, 2010 in the Marmara
88 Region. They concluded that cold air in the upper atmosphere, slow-moving quasi-
89 stationary trough and continuous moisture transfer from the warm Aegean Sea to the
90 surface low were the main mechanisms that led to intense storms.

91 Differently from the previous studies mentioned above, many severe precipitation
92 events frequently occur and generally conclude with flash floods and triggered landslides in
93 the eastern Black Sea (EBS) region of Turkey (Fig. 1). The EBS comprises the Black Sea
94 (BS) in the north and the eastern Anatolian Peninsula in the south. The underlying geology
95 of the EBS is generally consists of semi-permeable volcanic rocks which reduce infiltration
96 and enhance runoff production (Üçüncü et al., 1994). The north-eastern coastal parts of
97 Turkey, regions located on the windward slopes of the EBS facing the Black Sea, receives

mac baltaci 23/5/2017 12:10

Deleted:

mac baltaci 23/5/2017 12:10

Deleted: (southwestern Mediterranean Sea coast of Turkey)

mac baltaci 23/5/2017 12:12

Deleted: a flood at Marmara from September 7 to 10, 2009

mac baltaci 16/5/2017 01:34

Deleted: a

mac baltaci 23/5/2017 12:14

Deleted: The strata of the EBS are generally made of semi-permeable volcanic rocks, which prevent the rainfall from percolation and force the water to flow as runoff

mac baltaci 23/5/2017 12:16

Deleted: Located in the north-eastern coast of Turkey, this unique area has the highest mean annual precipitation records (above 2200 mm)

113 more than 2000 mm of annual precipitation which is the wettest part of the country. The
114 large mountainous area which extends through the Black Sea, and slope instability due to
115 steep gradients as well as intense rainfall result in flash floods and landslides and threaten
116 the settlements in the EBS region. In addition to all these topographical and meteorological
117 factors, commercial development and urbanization of the region (e.g. the cultivation of tea
118 on the sloping terrain instead of deep-rooted trees and illegal land-usage) facilitate the
119 flooding. Yüksek et al., (2013) have emphasized that 258 deaths and US \$500,000,000
120 economic losses occurred as a result of the 51 big floods in this basin from 1955 to 2005.
121 They briefly analyzed the hydro-meteorological role of selected nine floods in the region.
122 In one of the latest rainstorm events in the EBS, more than 135 mm of 24-h accumulated
123 rainfall in the Artvin surroundings (i.e. 144, 136 and 149 mm in Hopa, Arhavi and Borçka
124 stations, respectively) caused flash floods and landslides on August 24, 2015, resulting in
125 11 deaths and a million dollars worth of economic losses (Fig. 2). In spite of the several
126 negative impacts of flooding for the region and country, there are no detailed studies in the
127 literature which investigate the detailed meteorological role in the development of the
128 convective cells for the EBS. Therefore, the aim of this research is focused on this extreme
129 event, with the following main objectives: (a) to provide a detailed spatio-temporal
130 evaluation of rainstorms on 24 August 2015 that triggered the flash floods and landslides.
131 Daily and hourly precipitation measurements of the available meteorological stations were
132 used to understand temporal and spatial behavior of the rainstorm in the different
133 geographic elevations, (b) to improve our understanding of the meteorological features of
134 this extreme event by focusing on the relevant atmospheric synoptic conditions, satellite

mac baltaci 23/5/2017 12:18

Deleted: , which is parallel with the BS, and slope instability as well as intense rainfall result in flash floods and landslide events and threaten the settlements of the region

mac baltaci 20/5/2017 01:20

Deleted: s

mac baltaci 16/5/2017 01:38

Deleted: '

141 and radar images and physical mechanisms (e.g. sea surface temperature evolution) that
142 favored its development.

143

144 2. Data and Methodology

145 In order to evaluate the research results, precipitation, sea surface temperature, synoptic,
146 and atmospheric data are included in the study. To compare precipitation observations with
147 weather forecasts, three numerical weather prediction (NWP) model outputs were assessed.

148 2.1 Precipitation and sea surface temperature (SST) data

149 The eastern Black Sea region is well covered by automated meteorological stations. In
150 addition to the eight long-term stations in the region, 41 new automated meteorological
151 stations have been added since 2013. To present the high spatial resolution and to retrieve a
152 homogeneous dataset, hourly and daily precipitation data of 49 stations operated by Turkish
153 State Meteorological Service (TSMS) were used in the study (Fig.1). The main
154 characteristics of the stations are described in Table 1.

155 2.2 Synoptic and atmospheric data

156 The synoptic context of the extreme event of August 24, 2015 as well as the previous day,
157 atmospheric conditions was analyzed with NCEP/NCAR 2.5°X2.5° latitude/longitude
158 reanalysis data. To track the intense rainfall episodes, radar PPI (Plan Position Indicator)
159 images, which provided by TSMS, were used. Rainstorm development stages associated
160 with the flash flood were evaluated with Meteosat 10 images.

mac baltaci 16/5/2017 01:39
Deleted: y
mac baltaci 16/5/2017 01:39
Deleted: y
mac baltaci 16/5/2017 01:40
Deleted: as well as

mac baltaci 16/5/2017 01:41
Deleted: 's

165 **2.3 Numerical weather prediction (NWP) model outputs**

166 Operationally, one global and two regional NWP models are run regularly twice a day
167 (00:00 and 12:00 UTC) for the precipitation forecast by TSMS. In terms of the global
168 NWP, the horizontal grid resolution of ECMWF (European Centre for Medium-Range
169 Weather Forecasts) the IFS (Integrated Forecast System) covers almost 16 km and uses 91
170 vertical levels. For the regional weather forecasts, the Alaro meteorological model has been
171 designed to be run at convection-permitting resolutions. The key concept is in the
172 precipitation and cloud scheme called Modular Multiscale Microphysics and Transport
173 (3MT) developed by Gerard and Geleyn (2005), Gerard (2007), and Gerard et al. 2009. In
174 the usage of the Alaro by TSMS, whereas the outer domain has grid spacing of 10 km, the
175 inner domain has almost 5 km of grid spacing as well as 60 vertical levels.

176 The mesoscale NWP system of Non-hydrostatic Mesoscale Model (NMM) core of the
177 Weather Research and Forecasting (WRF) is developed by the National Oceanic and
178 Atmospheric Administration (NOAA)/National Centers for Environment Prediction
179 (NCEP), WRF-NMM is a fully compressible, non-hydrostatic mesoscale model with a
180 hydrostatic option (Janjic, 2003). The model uses a terrain-following hybrid sigma-pressure
181 vertical coordinate. The grid staggering is the Arakawa E-grid. The model uses a forward-
182 backward scheme for horizontally-propagating fast waves, an implicit scheme for
183 vertically-propagating sound waves, the Adams-Bashforth scheme for horizontal advection,
184 and the Crank-Nicholson scheme for vertical advection. The dynamics conserve a number
185 of first and second order quantities including energy and enstrophy. In the study, model has
186 a horizontal grid spacing of 30 km in its outer computational domain, and the inner domain

mac baltaci 16/5/2017 03:57
Deleted: In

mac baltaci 16/5/2017 03:58
Deleted: ,
mac baltaci 16/5/2017 04:03
Deleted:

mac baltaci 16/5/2017 03:29
Deleted: WRF (

mac baltaci 16/5/2017 03:30
Deleted:)

192 has a grid spacing of 10 km together with 46 vertical levels. To compare precipitation
193 forecasts of these models with the observation results, daily precipitation forecasts of the
194 models belonging on the last runtime for August 24, 2015, at 00:00 UTC outputs were
195 assessed.

mac baltaci 16/5/2017 03:41
Formatted: Font:Not Bold, Font color:
Black

196 3. Results and discussion

197 3.1 Precipitation climate of eastern Black Sea

198 The coastal part of the region is restricted by the EBS Mountain chain in the south and the
199 BS in the north (Fig.1). This mountain chain extends parallel to the Black Sea and has an
200 average altitude of 2000 m. It rises to 3973 m at its highest point (Eris et al., 2012). Apart
201 from the basic synoptic scale circulations such as continental polar and tropical air masses,
202 the region is also affected by orographic precipitation. Colder air masses are prevented by
203 the Caucasus Mountains (the highest point of Georgia) from the north; therefore, more dry
204 climates are seen in the south part of the region. The rain shadow effect on the lee side of
205 the mountainous area causes a more continental climate in the southern parts of the EBS
206 (Biyik et al., 2010). When compared with the other regions, highest winter and summer
207 precipitation totals are observed in this part of Turkey due to the interactions of synoptic
208 weather patterns and orographic lifting. (Unal et al., 2012). To better visualize the seasonal
209 precipitation variability in the EBS, long-term precipitation data from 1960 to 2014 were
210 extracted from the available eight meteorology stations (stations marked by stars in Table 1
211 were used for the climatological approach in Fig. 3). Five stations are located in the north
212 of the region. According to the results, mean annual precipitation (MAP) varies from 438

mac baltaci 23/5/2017 22:07
Deleted: is in
mac baltaci 23/5/2017 22:07
Deleted: with
mac baltaci 23/5/2017 22:07
Deleted: S

mac baltaci 20/5/2017 00:38
Deleted: moderate
mac baltaci 23/5/2017 22:09
Deleted: Lee side effects of the
mountainous area generate

mac baltaci 20/5/2017 00:47
Formatted: Font:12 pt
mac baltaci 20/5/2017 00:47
Formatted: Font:12 pt
mac baltaci 20/5/2017 00:47
Deleted: In terms of the precipitation
values, because of the interactions of weather
systems and the orographic uplifting, the
highest amount of precipitation is observed
during wet and dry seasons compared with the
other regions of the country

mac baltaci 20/5/2017 01:25
Deleted: change

226 mm in the south (Bayburt) to 2243 mm in the north (Hopa). This high spatial precipitation
227 variability generates different land cover terrain. Interestingly, the highest seasonal
228 precipitation amounts in the coastal areas were observed in the fall (SON) months. This can
229 be explained by the significance of MCS, flow directions and SST variations over EBS. In
230 the second wettest season (DJF), highest precipitation records were observed at Hopa, Rize,
231 and Pazar stations with the values 606, 636, and 550 mm, respectively.

232 3.2 Spatio-temporal variability of rainfall episodes

233 In Fig. 4a, spatial distribution of daily precipitation totals for August 24, 2015 was
234 extracted from 49 meteorological stations. It can be seen that three main cores of
235 precipitation are measured at the Arhavi, Hopa, and Borçka stations with the values of 135,
236 144, and 149 mm, respectively. In Hopa, 27% of the long-term mean of summer rainfalls
237 was recorded on this day. As a consequence of the intense daily rainfall episodes, these
238 three surrounding areas of Artvin district were the most influenced by flash floods and
239 landslides (i.e. Hopa, Arhavi, and Borçka). Among these stations, Hopa (33m altitude, no. 1
240 in Fig. 1b) is at the lowest altitude and is located in the north coastal part of Artvin city.
241 Borçka station is shown with an altitude of 190m (the second lowest altitude in Artvin, no.
242 7 in Fig. 1b). Another coastal station, Arhavi (290m altitude, no. 6 in Fig 1b), is located in
243 the northwest and has the third lowest altitude among all Artvin stations. Temporal
244 precipitation distribution of these selected stations was extracted as shown in Fig. 4b.
245 Rainstorms started in the evening (22:00 UTC) of August 23, 2015 and ended at the
246 midday on the following day. Hourly observations at the three stations showed the
247 torrential rains increased from 27 to 32 mm between 22:00 and 24:00 UTC on August 23,

mac baltaci 16/5/2017 01:46
Deleted: instead of the winter (DJF)
mac baltaci 16/5/2017 01:45
Deleted: in the coastal areas
mac baltaci 20/5/2017 01:26
Deleted: shown for the
mac baltaci 16/5/2017 01:47
Deleted: Nevertheless, the third highest seasonal precipitation totals in these stations are shown in JJA.

mac baltaci 16/5/2017 01:48
Deleted: ose

mac baltaci 23/5/2017 22:14
Deleted: The other seaside

mac baltaci 20/5/2017 01:29
Deleted: in
mac baltaci 16/5/2017 01:49
Deleted: to

258 thereafter suddenly dropping from 4 to 2 mm between 01:00 and 05:00 UTC on August 24.
259 Later, uninterrupted extreme rainstorms hit the north and coasts of the Artvin district.
260 According to the hourly rainfall observations, the highest precipitation amounts were
261 recorded at Hopa during the eight hours of the flash flood day (Fig. 4b). The maximum
262 daily precipitation value was observed with 144.3 mm in six hours (starting at 05:00 UTC
263 and ending at 11:00 UTC) in Hopa, and maximum hourly rainfall measured 51.5 mm at
264 09:00 UTC. In Arhavi, daily total precipitation was 135.5 mm and reached a maximum
265 value at 00:00 UTC with 32.4 mm. In Borçka, while daily precipitation amounts were
266 higher (148.9 mm) than at Hopa and Arhavi, peak values of hourly precipitation intensities
267 were lower. According to the results from these three stations, hourly precipitation reached
268 a maximum value at 09:00 UTC in the low altitudes of the region; this implies that the
269 precipitation was much lower in the upper sectors of the mountainous area.

270 3.3 Synoptic overview

271 This section treats the atmospheric circulation and associated physical mechanisms that
272 were responsible for the flash flood in the region. In order to better evaluate the
273 phenomenology of the event, pre-existing synoptic conditions starting from August 23 were
274 investigated. At 00:00 UTC on August 23, the summer Asian monsoon low extends to the
275 eastern Black Sea (Fig. 5a). During the summer months, in consequence of the excessive
276 surface heating over the arid regions of the Middle East, the monsoon low expands
277 westward and generates the Persian trough (Alpert et al. 2004; Saaroni et al. 2010), which
278 extends to Turkey, forming a thermal low over the eastern Mediterranean (Tyrlis et al.
279 2015). Besides the surface synoptic conditions, low-level moisture convergence, specific

mac baltaci 16/5/2017 01:50
Deleted: to

mac baltaci 16/5/2017 01:50
Deleted: 2

mac baltaci 16/5/2017 01:50
Deleted: 4

mac baltaci 20/5/2017 01:29
Deleted: station

mac baltaci 16/5/2017 01:51
Deleted: Daily precipitation record

285 humidity content and geopotential height values of 850 hPa were extracted. It is known that
286 low-level moisture convergence is a good indicator for large-scale precipitation (e.g.
287 Frago et al. 2012), and eastern Turkey (Azerbaijan) has good synoptic precipitation
288 conditions. In the upper levels, interaction between weak ridge over northern Africa and
289 trough over the Aegean Sea (because of the upper-level cold low over central Europe)
290 concludes with southwesterly winds over the Artvin district (Fig. 5c).

291 On August 24 at 00:00 UTC, a high pressure center (HPC) over northern Russia moved to
292 the south, located around 30° E, 60° N. While the cyclone remained almost stationary, a
293 new cut-off cyclone occurred over the EBS (Fig. 5d). Thus, high northeasterly winds
294 brought moisture from the Black Sea to the eastern coasts of Turkey (Fig. 5e). As a result,
295 deep precipitation areas were observed over these regions according to the low-level
296 moisture convergence results. In the upper level chart (500 hPa), shifting cold core of upper
297 level high to the south cause the moving of mid-latitude low to the west, and, thus, south-
298 westerly winds turn into the westerly together with a decrease in temperature from -7.5 °C
299 to -10 °C (Fig. 5f).

300 At the start of the rainstorm (August 24, 06:00 UTC), similar surface and upper-level large-
301 scale circulations appeared compared with the midnight synoptic conditions (Figs 6a and
302 6c). Strong moisture convergence zones were detected over the flash-flood region (Fig. 6b).
303 For this reason, thermodynamic analysis was needed to better understand the evaluation of
304 physical mechanisms that developed severe precipitation. Hence, as a consequence of
305 analyzing the nearest radiosonde measurements from Samsun station (41.34 °N, 36.25 °E),

mac baltaci 16/5/2017 01:52
Deleted: t of
mac baltaci 16/5/2017 01:56
Deleted: the presence of a
mac baltaci 16/5/2017 01:57
Deleted: h
mac baltaci 16/5/2017 01:57
Deleted: the axis

mac baltaci 16/5/2017 01:58
Deleted: ;
mac baltaci 23/5/2017 22:20
Deleted: ing
mac baltaci 23/5/2017 22:20
Deleted: of

313 instability indices such as CAPE (Convective Available Potential Energy) and LI (Lifted
314 Index) showed that there was no strong convective activity before and during the rainstorm
315 (not shown).

316 In order to follow the distribution convective cells and cloud droplets in a large area, it was
317 necessary to use satellite and radar image data.

318 3.4 Satellite and radar images

319 Repeated temporal resolution is an excellent tool for understanding the spatial distribution
320 of the convective cells. Therefore, SEVIRE (Spinning Enhanced Visible and Infrared
321 Imager) MSG (Meteosat Second Generation) outputs were used to examine the atmospheric
322 conditions on August 24 at 06:00 UTC. It is known that ‘convective storms RGB’ product
323 visualizes the particle size features of high-level cloud tops with good contrast (Kerkmann
324 et al., 2006). Whereas yellowish cloud tops indicate opaque ice clouds with small particles,
325 high-level opaque ice clouds with large particles are shown as reddish. The RGB product in
326 Fig. 7a was produced by assigning the brightness temperature difference (BTD) 6.2-7.3
327 values as the red component, the BTD 3.9-10.8 as the green component, 1.6-0.6 as the blue
328 component. In Fig. 7a, numerous convective storms with large ice particles are shown over
329 the EBS. On the other hand, more intense storms were observed over the land areas such as
330 Georgia and this implies the storm intensity. Separately, SYNOP observations indicate that
331 southerly winds over the coast of the EBS stations met with humid northerly flows
332 throughout the seaside area. If the land (21 °C) and sea surface temperatures (SSTs) were
333 sufficiently different, the convective instability and storm severity could have increased

mac baltaci 20/5/2017 01:31

Deleted: during

mac baltaci 20/5/2017 01:31

Deleted: before

mac baltaci 23/5/2017 22:23

Deleted: over the land areas (e.g. Georgia)

mac baltaci 23/5/2017 22:23

Deleted: yellowish particles

mac baltaci 23/5/2017 22:23

Deleted: are

mac baltaci 16/5/2017 02:01

Deleted: 's

341 with time. As seen in Fig. 7b, high PPI (Plan Position Indicator) reflectivity values from the
342 radar image showed that two cores of the extreme precipitation were over the Hopa and
343 Çayeli sub-basins.

344 3.5 Sea surface temperature (SST) analysis over Black Sea

345 The influence of SSTs on precipitation over Turkey was investigated in detail by Bozkurt
346 and Sen (2011). They found that increased SSTs led to increased precipitation of the
347 peninsula especially downwind of the sea. Later, Kömüşçü and Çelik (2013) explained that
348 warm Aegean SST is one of the significant causes of the development of rainstorms. In this
349 study, exploring the role of Black Sea surface temperatures on storm development, long-
350 term (1982-2015) means of August SSTs were extracted for the BS using NOAA High
351 Resolution SST data (provided by NOAA/OAR/ESRL PSD, Reynolds et al. 2007). As seen
352 in Fig. 8a, cold SSTs of the BS were north of the latitude of 44 °N. The warmest pool of the
353 BS in the eastern BS and SSTs exceeded 27 °C in this month. During the day of the
354 extreme event, spatial distribution of the SSTs indicates negative anomaly values in north
355 of 44 °N latitudes (Fig. 8b). The EBS region has the highest SST anomalies and 1.5 °C
356 higher SST variations compared with the August means for the EBS.

357 3.6 Forecasting tools: Numerical Weather Prediction (NWP) models

358 According to the ECMWF daily precipitation product, spatial coverage of the maximum
359 daily precipitation values (over 160 mm) is shown in the northern Rize and northwestern
360 Artvin cities (Fig. 9a). Compared with the model output (Fig. 4a), station observations were
361 clearly underestimated in northern Rize. On the other hand, model predictions for the

mac baltaci 20/5/2017 01:33

Deleted: detail

mac baltaci 20/5/2017 01:35

Deleted: above

mac baltaci 20/5/2017 01:37

Deleted: the upper

mac baltaci 20/5/2017 01:37

Deleted: are

366 | Arhavi and Borçka settlements, except Hopa, were good. With regard to the Alaro model
367 | results, the highest daily precipitation totals were well predicted only for Hopa district at
368 | 150 mm (Fig. 9b). Although precipitation forecasts of this limited-area model described
369 | Hopa well, the other two flood regions were not well predicted. Optimum spatial coverage
370 | of the daily precipitation forecasts is shown in the mesoscale WRF outputs (Fig. 9c). The
371 | problem with this model is the underestimated forecasts compared with the observation
372 | data. In TSMS, meteorologists merge the outputs of these models (the so-called “poor man
373 | ensemble”) with their own experience and provide quantitative precipitation forecasts for
374 | the alert sub-regions in predefined time windows. As a consequence of this subjective
375 | prediction, TSMS and its regional weather forecast offices issued alert messages related to
376 | natural hazards including severe precipitation events. These organizations also carry the
377 | responsibility for nowcasting and monitoring rainfall events. According to the main alert on
378 | August 23, 2015 at 09:00 UTC prepared by TSMS Weather Forecast Centre, very intense
379 | precipitation between 51 and 100 mm was predicted at the Rize, Artvin, and Trabzon
380 | districts within 12 hours of August 24. The authorities and the public were alerted to the
381 | risk of flash flood, lightning, and landslide events.

382 | 4. CONCLUSION

383 | This paper investigated the meteorological role in an extraordinary rain event over Artvin.
384 | The flooding event on August 24, 2015 that hit the Artvin area has been analyzed from a
385 | meteorological perspective. A large amount of precipitation fell in an area of a few square
386 | kilometers with high intensity in about 6 to 7 hours, and NWP models cannot well predict
387 | such extreme events. Although alert messages were prepared by TSMS on August 23 at

mac baltaci 16/5/2017 02:02

Deleted: 's

mac baltaci 16/5/2017 02:03

Deleted: give

390 09:00 UTC, 11 people died and infrastructures, buildings, private property and public
391 goods were damaged as a result of the flash flood.

392 According to the synoptic conditions, when the summer monsoon frontal system extended
393 to eastern Anatolia, its activity was enhanced. On the other hand, because of the depressive
394 effect of the Siberian high from the north, a cut-off low occurred over the eastern Black
395 Sea. As a result, a slow-moving quasi-stationary cut-off low over the Black Sea increased
396 the SSTs and more moisture was transported from the sea to the atmosphere. Thus, strong
397 moisture convergence at low-levels (850 hPa) was observed over Artvin city. Moreover,
398 warm humid northerly airs from the Black Sea and relatively cool southerly flows (21 °C)
399 over the land areas increased the instability conditions and redevelopment of the convective
400 cells over the same region enhanced the rainfall intensity.

401 The synoptic and atmospheric descriptions give better knowledge of the mesoscale
402 convective systems and the mechanisms driving torrential rains in the EBS. It is hoped that
403 more detailed studies will be performed on synoptic development leading to extreme
404 summer precipitation events in EBS.

405 **References**

- 406 Alpert, P., Osetinsky, I., Ziv, B. and Shafir, H.: A new seasons definition based on
407 classified daily synoptic systems: an example for the eastern Mediterranean.
408 International Journal of Climatology 24:1013–1021, 2004.
- 409 Aronica, G.T., Brigandi, G., Marletta, C. and Manfre, B.: Hydrological and hydraulic
410 analysis of the flash flood event on 25 October 2007 in North-Eastern part of Sicily,
411 Italy. Proceedings of Floodrisk 2008, Oxford (UK), 2008.
- 412 Arpe, K., Dümenil, L. and Giorgetta, M. A.: Variability of Indian Monsoon in the
413 ECHAM3 Model: sensitivity to sea surface temperature, soil moisture, and stratospheric
414 quasi-biennial oscillation. Journal of Climate 11:1837–1858, 1998.

mac baltaci 16/5/2017 02:05

Deleted: This paper investigated the meteorological role in an extraordinary rain event over Artvin.

- 418 Biyik, G., Unal, Y. S. and Onol, B.: Assessment of Precipitation Forecast Accuracy over
 419 Eastern Black Sea Region using WRF-ARW. European Geosciences Union General
 420 Assembly, Vienna, 02.05.2010–07.05.2010, 2010.
- 421 Borga, M., Boscolo, P., Zanon, F. and Sangati, M.: Hydrometeorological Analysis of the 29
 422 August 2003 Flash Flood in the Eastern Italian Alps. *Journal of Hydrometeorology* 8:
 423 1049–1067, 2007.
- 424 Bozkurt, D. and Sen, O. L.: Precipitation in the Anatolian Peninsula: sensitivity to
 425 increased SSTs in the surrounding seas. *Climate Dynamics* 36: 711–726, 2011.
- 426 Delrieu, G., Nicol, J., Yates, E., Kirstetter, P. E., Creutin, J. D., Anquetin, S., Obled, C. H.,
 427 Saulnier, G. M., Ducrocq, V., Gaume, E., Payrastré, O., Andrieu, H., Ayrat, P. A.,
 428 Bouvier, C., Neppel, L., Livet, M., Lang, M., Parent du-Châtelet, J., Walpersdorf, A.
 429 and Wobrock, W.: The catastrophic flash-flood event of 8–9 September 2002 in the
 430 Gard region, France. A first case study for the Cévennes–Vivarais mediterranean
 431 hydrometeorological observatory. *Journal of Hydrometeorology* 6 (1):34–52, 2005.
- 432 Eris, E. and Agiralioglu, N.: Homogeneity and Trend Analysis of Hydrometeorological
 433 Data of the Eastern Black Sea Region, Turkey. *Journal of Water Resource and
 434 Protection* 4:99–105, 2012.
- 435 Fragoso, M., Trigo, R. M., Pinto, J. G., Lopes, S., Lopes, A., Ulbrich, S. and Magro, C.:
 436 The February 2010 Maderia flash-floods: synoptic analysis and extreme rainfall
 437 assessment. *Natural Hazards and Earth System Sciences* 12:715–730, 2012.
- 438 Gaume, E., Bain, V. and Bernardara, P.: Primary Flash flood Data, Work Package 1 Report
 439 for HYDRATE, EC Project No. GOCE-CT-2004-505420, 2008.
- 440 [Gerard, L.: An integrated package for subgrid convection, clouds and precipitation
 441 compatible with the meso-gamma scales. *Quarterly Journal of the Royal
 442 Meteorological Society* 133:711–730, 2007.](#)
- 443 [Gerard, L. and Geleyn J. F.: Evolution of a subgrid deep convection parameterization in a
 444 limited area model with increasing resolution. *Quarterly Journal of the Royal
 445 Meteorological Society* 131:2293–2312, 2005.](#)
- 446 [Gerard, L., Piriou J. M., Brozkova, R., Geleyn, J. F. and Banciu, D.: Cloud and
 447 precipitation parameterization in a meso-gamma-scale operational weather prediction
 448 model. *Monthly Weather Review* 137: 3960–3977, 2009.](#)
- 449 Huet, Ph., Martin, X., Prime, J-L., Foin, P., Laurain, C. I. and Cannard, Ph.: Retour
 450 d’expériences des crues de septembre 2002 dans les départements du Gard, de
 451 l’Hérault, du Vaucluse, des bouches du Rhône, de l’Ardèche et de la Drôme,
 452 Inspection générale de l’Environnement, Paris, France, 124 pp, 2003.
- 453 Janicot, S., Harzallah, A., Fontaine, B. and Moron, V.: West African monsoon dynamics
 454 and Eastern Equatorial Atlantic and Pacific SST anomalies (1970-1988). *Journal of
 455 Climate* 11:1874–1882, 1998.

- 456 | [Janjic Z. I.: A nonhydrostatic model based on a new approach. *Meteorology and*](#)
457 | [Atmospheric Physics 82: 271–285, 2003.](#)
- 458 Kerkmann, J., Lutz, H. J., König, M., Prieto, J., Pylkko, P., Roesli, H. P., Rosenfeld, D. and
459 Zwatz-Meise, G.: 20060 MSG Channels, Interpretation Guide, Weather, surface
460 Conditions and Atmospheric Constituents. Available online at
461 http://oiswww.eumetsat.org/WEBOPS/msg_interpretation/index.html, 2006.
- 462 Kotroni, V., Lagouvardos, E., Defor, S., Dietrich, F., Porcu, C., Medaglia, C. M. and
463 Demirtas, M.: The Antalya 5 December 2002 Storm: Observations and Model
464 Analysis. *Journal of Applied Meteorology and Climatology* 45:576–590, 2006.
- 465 Kömüşçü, A. Ü., Erkan, A. and Çelik, S.: Analysis of Meteorological and Terrain Features
466 Leading to the İzmir Flash Flood, 3–4 November 1995. *Natural Hazards* 18:1–25,
467 1998.
- 468 | Kömüşçü, A. Ü. and Çelik, S.: Analysis of the Marmara flood in Turkey, 7–10 September
469 2009: an assessment from hydrometeorological perspective. *Natural Hazards* 66:781–
470 808, 2013.
- 471 LLasat, M. C., De Batlle, J., Rigo, T. and Barriendos, M.: Las Inundaciones del 10 de Junio
472 del 2000 en Catalana. *Revista Ingenieria del Agua* 8: 53–66, 2001.
- 473 Maracchi, G., Crisci, A., Grifoni, D., Gozzini, B. and Meneguzzo, F.: Relationships
474 between convective events and sea surface temperature anomalies in coastal regions of
475 the Mediterranean. Proceedings of the EuroConference on global change and
476 catastrophe risk management: flood risks in Europe. Laxenburg, Austria, 1999.
- 477 Messenger, C., Gallee, H. and Bresseur, O.: Precipitation sensitivity to regional SST in a
478 regional climate simulation during the West African monsoon for two dry years.
479 *Climate Dynamics* 22:249–266, 2004.
- 480 Milelli, M., Llasat, M. C. and Ducrocq, V.: The cases of June 2000, November 2002 and
481 September 2002 as examples of Mediterranean floods. *Natural Hazards and Earth*
482 *System Sciences* 6:271–284, 2006.
- 483 Rebora, N., Molini, L., Casella, E., Comellas, A., Fiori, E., Pignone, F., Siccardi, F.,
484 Silvestro, F., Tanelli, S. and Parodi, A.: Extreme Rainfall in the Mediterranean: What
485 Can We Learn from Observations?. *Journal of Hydrometeorology* 14: 906–922, 2013.
- 486 Reynolds, R. W., Smith, T. M., Liu, C., Chelton, D. B., Casey, K. S. and Schlax, M. G.:
487 Daily high-resolution-blended analyses for sea surface temperature. *Journal of Climate*
488 20:5473–5496, 2007.
- 489 Saaroni, H., Ziv, B., Osetinsky, I. and Alpert, P.: Factors governing the interannual
490 variation and the long-term trend of the 850 hPa temperature over Israel. *Quarterly*
491 *Journal of the Royal Meteorological Society* 136:305–318, 2010.
- 492 Silvestro, F., Gabellani, S., Giannoni, F., Parodi, A., Rebora, N., Rudari, R. and Siccardi,
493 F.: A hydrological analysis of the 4 November 2011 event in Genoa. *Natural Hazards*
494 and *Earth System Sciences* 12:2743–2752, 2012.

mac baltaci 12/6/2017 13:40

Deleted: t

496 Tyrllis, E., Tymvios, F. S., Giannakopoulos, C. and Lelieveld, J.: The role of blocking in the
497 summer 2014 collapse of Etesians over the eastern Mediterranean. *Journal of*
498 *Geophysical Research: Atmospheres* 120: doi:10.1002/2015JDO23543, 2015.

499 Unal, Y. S., Deniz, A., Toros, H. and Incecik, S.: Temporal and spatial patterns of
500 precipitation variability for annual, wet, and dry seasons in Turkey. *International*
501 *Journal of Climatology* 32:392–405, 2012.

502 Üçüncü, O., Önsoy, H. and Yüksek, Ö.: A Study on the environmental effects of 20 June
503 1990 flood in Trabzon and its neighborhood, Turkey. 2nd International Conference on
504 River Flood Hydraulics. York, England, 1994.

505 Yüksek, Ö., Kankal, M. and Üçüncü, O.: Assessment of big floods in the Eastern Black Sea
506 Basin of Turkey. *Environmental Monitoring and Assessment* 185:797–814, 2013.

507

508

509

510

511

512

513

514

515

516

517

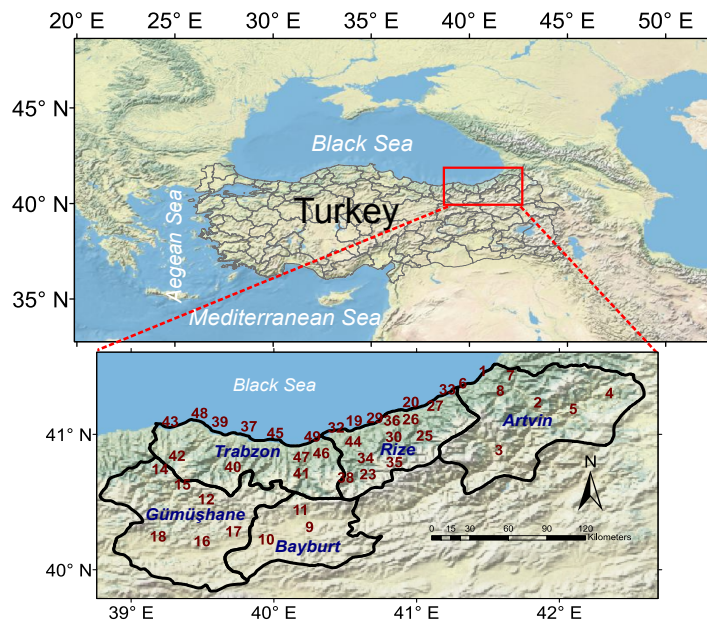
518

519 **Table 1 :** Description of 49 meteorological stations in the study. Stations marked by stars
520 were used for the climatological approach.

Station No.	Station Code	Station name	Longitude (E)	Latitude (N)	Altitude (m)	23 Aug 2015 precip. (00-00 UTC)	24 Aug 2015 precip. (00-00 UTC)
1	17042	Hopa*	41.4330	41.4065	33	55.3	144.3
2	17045	Artvin*	41.8187	41.1752	613	0	1.4
3	18216	Yusufeli	41.5464	40.8228	601	0	4.4
4	18217	Savsat	42.3206	41.2433	1125	0	24.4
5	18218	Ardanuc	42.0653	41.1267	577	0	11.6
6	18554	Arhavi	41.2928	41.3166	290	22.4	135.5
7	18555	Borcka	41.6281	41.3750	190	35.8	148.9
8	18556	Murgul	41.5564	41.2617	565	0.2	42.5
9	17089	Bayburt*	40.2207	40.2547	1584	0.4	0
10	18219	Demirozu	39.8858	40.1639	1757	0	0
11	18557	Aydintepe	40.1294	40.3817	1600	0.6	0
12	17088	Gumushane*	39.4653	40.4598	1216	0.1	0
13	17696	Torul (Zigana kayak m)	39.4037	40.6413	2050	0	0
14	18226	Kurtun	39.1456	40.6825	739	0	1.5
15	18227	Torul	39.2989	40.5686	1009	0	0
16	18228	Kelkit	39.4361	40.1506	1483	0	0
17	18564	Kose	39.6578	40.2217	1635	0.1	0
18	18565	Siran	39.1289	40.1856	1490	3.3	0
19	17040	Rize*	40.5013	41.0400	3	28.3	26.2
20	17628	Pazar*	40.8993	41.1777	78	35.8	49
21	17713	Camlihemsin (Ayder FI)	41.1103	40.9518	1354	1.6	18.8
22	17741	Ikizdere (Sivrikaya)	40.7106	40.6711	1926	0	7.8
23	17757	Ikizdere (Derekoy)	40.5989	40.7258	970	0.4	37.2
24	17761	Kalkandere	40.4400	40.9278	138	5.7	75.1
25	17765	Camlihemsin	40.9942	41.0125	390	2.8	32.1
26	17769	Hemsin	40.8992	41.0503	307	22.3	21.9
27	17772	Ardesen (Yesiltepe)	41.0703	41.1528	573	0.4	0
28	17775	Iyidere (Fidanlik)	40.3319	40.9835	6	21.1	29.8
29	17781	Cayeli (Teias)	40.7417	41.0603	54	31.9	30.9
30	17785	Cayeli (Kaptanpasa)	40.7789	40.9583	483	15.2	54.1
31	17800	Guneyusu	40.6083	40.9897	124	31.1	58.8
32	18566	Derepazari	40.4289	40.9897	397	20.1	38
33	18567	Findikli	41.1556	41.2703	190	24.7	62.3
34	18568	Rize (Andon)	40.5825	40.8711	615	12.6	88.8
35	18569	Ikizdere (Cimil)	40.7828	40.7333	2020	0.5	16.3
36	18905	Cayeli (Bakir)	40.7669	41.0408	100	32.3	56.5
37	17037	Trabzonbolge*	39.7649	40.9985	25	2.6	17.4
38	17569	Caykara (Uzungol)	40.4435	40.6193	1114	1.6	11.6
39	17626	Akcaabat*	39.5615	41.0325	3	1	36.6
40	17714	Macka (Altindere sume.)	39.6532	40.6985	1030	0.4	1.6
41	18229	Duzkoy	40.1339	40.7708	622	0.7	8.2
42	18230	Tonya (Kalincam)	39.2617	40.7803	1100	0	7.1
43	18231	Besikduzu	39.2144	41.0328	374	12	30.1

44	18232	Hayrat (Pazaronu)	40.4961	40.8858	367	17.6	43
45	18233	Arsin	39.9497	40.9486	169	0	14.5
46	18570	Dernekpazari	40.2719	40.7997	721	7	9.7
47	18571	Koprubasi (Beskoy)	40.1339	40.7710	975	14	17.3
48	18573	Carsibasi (Yoroz)	39.4208	41.0950	370	1.2	47.8
49	18574	Surmene (Denizbilimleri)	40.2097	40.9231	5	49.5	33.8

521
522
523
524
525
526
527
528
529
530
531
532
533
534
535
536
537
538
539
540
541
542
543
544
545
546
547
548
549
550
551
552
553

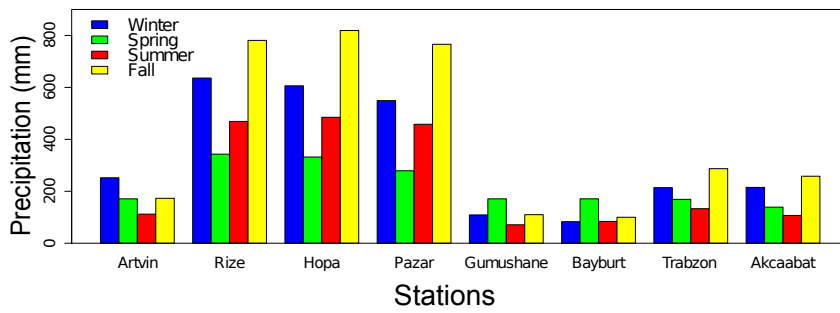


554 **Figure 1.** The eastern Black Sea Region included city names and borders and 49 automated
 555 meteorological stations (Descriptions of the station numbers are explained in Table 1). The
 556
 557 outset shows location of the region in Turkey.

558
 559
 560
 561
 562
 563
 564
 565
 566
 567
 568
 569
 570
 571
 572

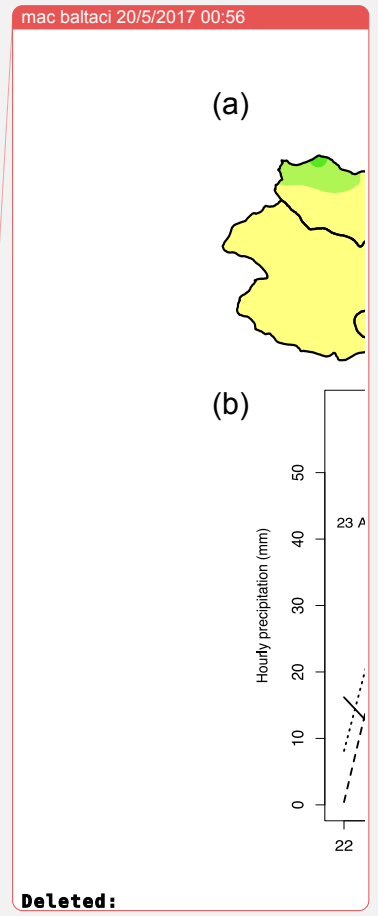
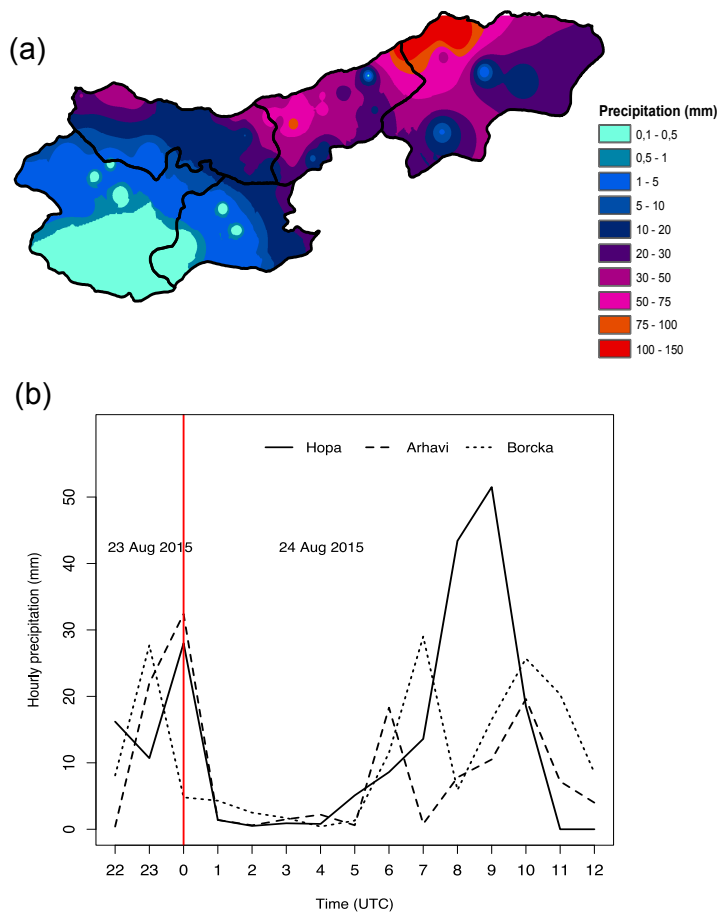


573
 574 **Figure 2.** Photos showing the destructive effects of the 24 August 2015 flash-floods and
 575 landslides in: **(a)** Hopa city centre flash-flood and **(b)** landslide in Hopa



576
 577 **Figure 3.** Long-term (1960-2014) mean of the seasonal precipitation amounts related to the
 578 eight meteorological stations in the EBS.

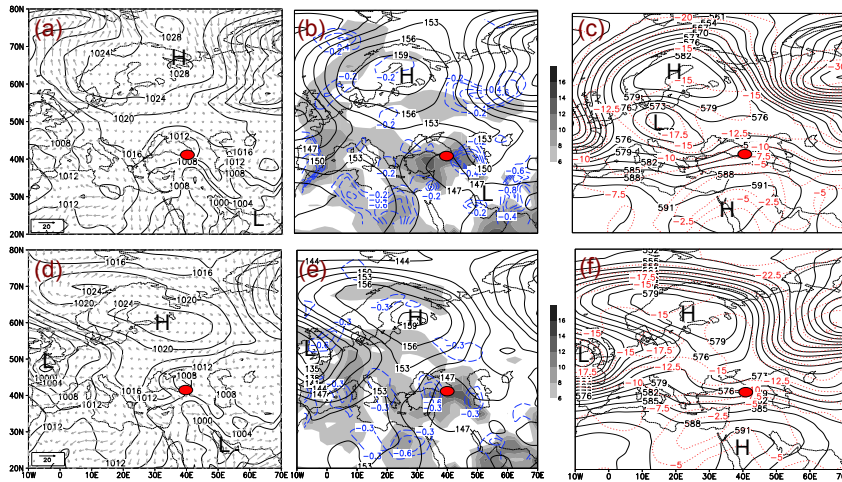
579
 580
 581
 582
 583



584
 585 **Figure 4.** (a) Total daily precipitation in the eastern Black Sea (00:00-24:00 UTC), 24
 586 August 2015. The map is based on data from the same meteorological stations represented
 587 in Fig. 1 (station names are listed in Table 1). (b) Hourly evolution of the 24 August 2015
 588 rainstorm in Artvin, in three selected stations representing flash-flood regions

589

591
592
593



594 **Figure 5.** (a) Sea level pressure chart (lines, units in hPa) and surface winds (arrows, units
595 in m s^{-1}). (b) Geopotential height field (units in dm), specific humidity contents (shaded in
596 colors, units in g kg^{-1}), and moisture convergence values (dashed lines, removed positive
597 values) of the 850-hPa level. (c) Geopotential height field (units in dm), and temperature
598 values (dashed red lines in $^{\circ}\text{C}$) of the 500-hPa level. Synoptic charts are belonging to the 23
599 August 2015, 00:00 UTC. The data of surface, lower and upper levels are derived from
600 NCEP/NCAR Reanalysis. Red dot marks the studied region. (d) same as (a), (e) same as
601 (b), (f) same as (c), but for 24 August 2015, 00:00 UTC.

603
604

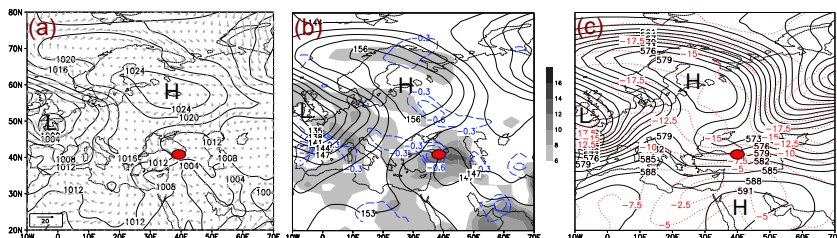
mac baltaci 23/5/2017 22:30

Deleted: 10^{-3} k

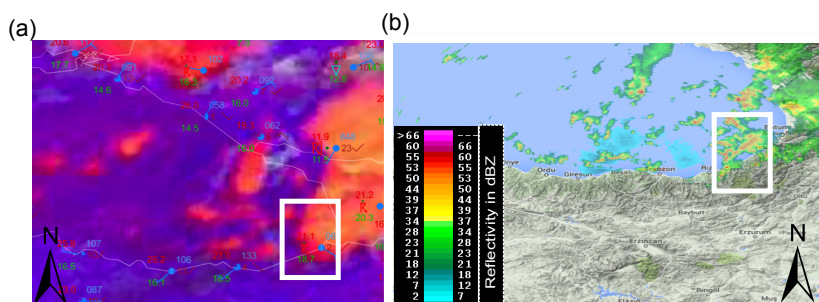
mac baltaci 16/5/2017 02:07

Deleted: ,

607



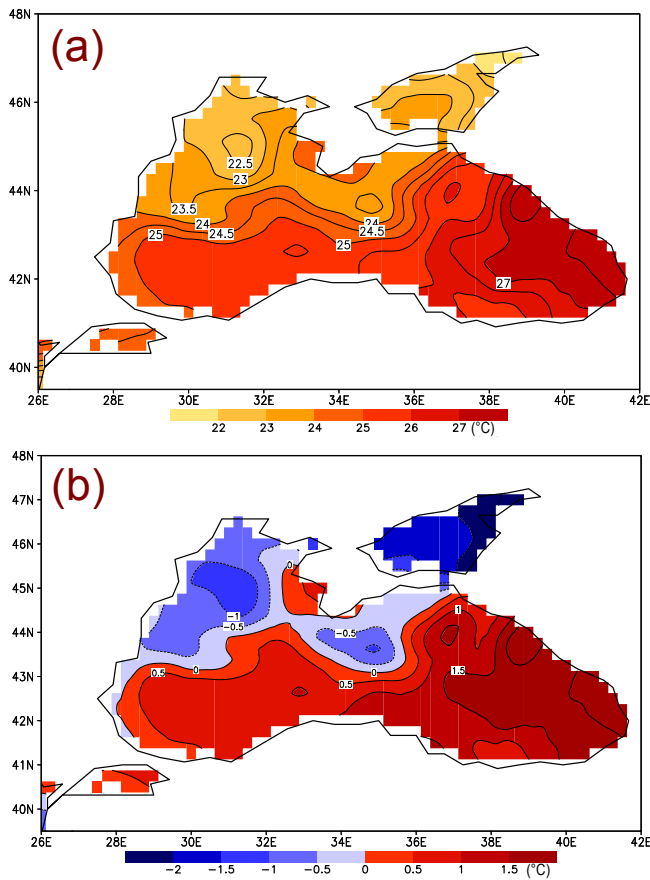
608
609 **Figure 6.** (a) same as Fig. 5(a), (b) same as Fig. 5(b), (c) same as Fig. 5(c), but for 24
610 August 2015, 06:00 UTC.



611
612 **Figure 7.** Satellite and radar images on 24 August 2015, 06:00 UTC. (a) Convective storm
613 RGB product from SEVIRE MSG (Meteosat Second Generation) together with SYNOP
614 observations. (b) Radar PPI (Plan Position Indicator) image of the EBS region. Sources: (a)
615 EUMETRAIN (<http://www.eumetrain.org/>) (b) Turkish State Meteorological Service
616 (www.mgm.gov.tr)

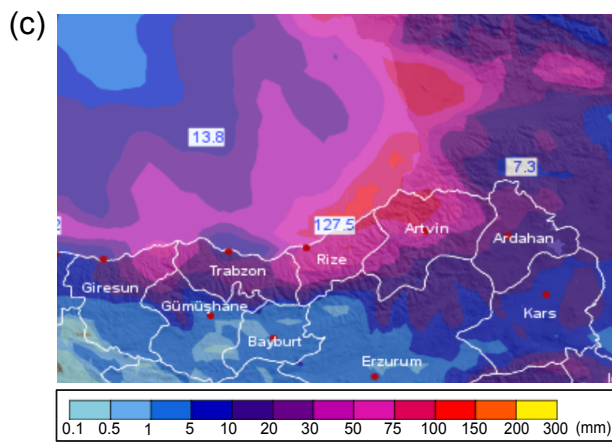
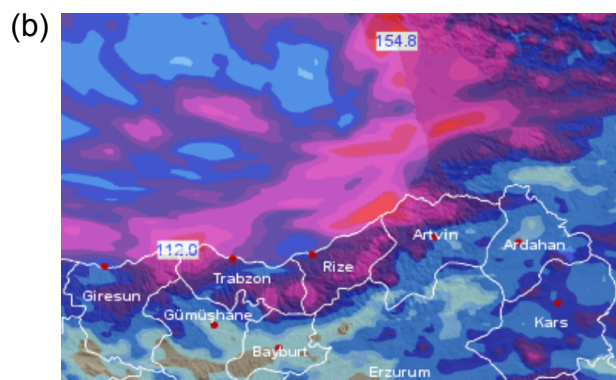
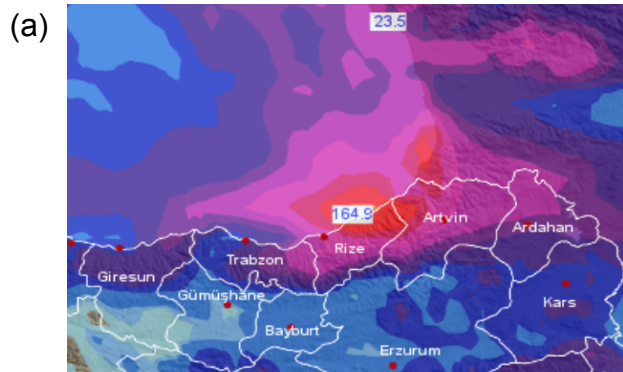
617
618

mac baltaci 20/5/2017 01:47
Deleted: ... [1]



621
 622 **Figure 8. (a)** Spatial distribution of the long-term (1960-2014) mean of August sea surface
 623 temperatures (SSTs) over the Black Sea. **(b)** Anomaly values of the 24 August daily mean
 624 SSTs when compared with long-term August mean SSTs. The SST Reanalysis data are
 625 derived from NOAA High Resolution SST (from their website is
 626 <http://www.esrl.noaa.gov/psd/>).

mac baltaci 20/5/2017 01:44
 Deleted: a
 mac baltaci 20/5/2017 01:45
 Deleted: a
 mac baltaci 20/5/2017 01:45
 Deleted: a
 mac baltaci 20/5/2017 01:45
 Deleted: is



632 **Figure 9.** Numerical Weather Prediction (NWP) precipitation forecasts for the 24-h daily
633 precipitation totals belonging to the 24 August 2015 in the EBS region, **(a)** for ECMWF **(b)**
634 for ALARO and **(c)** for WRF. Sources: (a-c) Turkish State Meteorological Service (TSMS)

635

mac baltaci 20/5/2017 01:46

Deleted: .